

# NaNu: Proposal for a Neutrino Experiment at the SPS Collider located at the North Area of CERN

Friedemann Neuhaus, Matthias Schott\*, and Rainer Wanke

Institute of Physics and PRISMA<sup>+</sup> Cluster of Excellence, Johannes Gutenberg University, Mainz, Germany

\* Corresponding author: matthias.schott@cern.ch

**Abstract.** Several experiments have been proposed in the recent years to study the nature of tau neutrinos, in particular aiming for a first observation of tau anti-neutrinos, more stringent upper limit on its anomalous magnetic moment as well as new constrains on the strange-quark content of the nucleon. We propose here a new low-cost neutrino experiment at the CERN North area, named NaNu (North Area NeUtrino), compatible with the realization of the future SHADOWS and HIKE experiments at the same experimental area.

## Contents

1	Introduction . . . . .	1
2	Detector Concept . . . . .	1
3	Neutrino Fluxes . . . . .	2
4	Detector Simulation and Neutrino Identification . . . . .	3
5	Expected Physics Reach . . . . .	5
6	Estimated Costs . . . . .	5
7	Summary . . . . .	5

## 1 Introduction

Within the SM, the neutrino sector is still the least understood and key questions, e.g. on the origin of the neutrino masses, are still not answered. Several new neutrino experiments are currently in preparation or just have started to take data [1]. A particular interesting development are new experiments at colliders, e.g. FASER [2] and SND@LHC [3], which aim for neutrino cross-section measurements in a new energy regime. Of particular interest are tau neutrinos, since the study of their properties are limited to nine  $\nu_\tau$  events observed at DONUT [4] and ten  $\nu_\tau$  candidate events at Opera [5]. The existence of anti-tau neutrinos has so far never been experimentally confirmed, making this the last missing particle within the SM. In fact, a huge number of tau- and anti-tau neutrinos could be produced in beam-dump experiments, where energies are high enough to produce  $D_s^\pm$  mesons, which subsequently decay via  $D_s \rightarrow \tau\nu_\tau$  with a branching fraction of about 5% [6]. Originally, the SHiP collaboration suggested a dedicated neutrino detector to study such tau-neutrino events, with a convincing physics case [7–9]. In this work, we propose a cost-efficient alternative neutrino detector, NaNu (North Area NeUtrino detector), which can be realized in-between the future SHADOWS and the HIKE experiments, as schematically shown in Figure 1. The planned SHADOWS experiment [10] at CERN

is one possible realization of a beam dump experiment, located at the CERN North Area next to the SPS collider aiming for the search of dark matter and hidden particles. The SHADOWS detector is about 35 m long and 2.5 m wide, placed about 1 m off-axis and 14 m after the beam dump itself, where a 400 GeV proton beam provides  $5 \times 10^{19}$  protons on target during a 4-year data-taking period between 2028 and 2032. The concept of SHADOWS foresees also the realization of the HIKE Experiment [11], which will be located about 50 m downstream of SHADOWS and will study extremely rare kaon decays.

In this work, we first discuss a preliminary NaNu detector concept, followed by an estimate on the neutrino fluxes, the identification of neutrino signatures as well as the physics reach and a cost estimate.

## 2 Detector Concept

The NaNu detector concept aims for a cost-efficient design using existing components and well established technologies. A schematic drawing of the NaNu detector is shown in Figure 2, showing its four major components, namely the magnetic system, the emulsion target, the active trigger system as well as the muon spectrometer. We suggest reusing an existing dipole magnet at CERN with gap dimensions of  $50 \times 100 \times 100$  cm<sup>3</sup> and a magnetic field strength of 1.4 T generated by a current of 2500 A. The transverse plane of the NaNu detector, facing the interaction point has therefore a size of  $50 \times 100$  cm<sup>2</sup>. The emulsion target is designed with transverse size of  $40 \times 50$  cm<sup>2</sup> and a depth of 80 cm, hence leaving 20 cm space downstream of the magnetic field.

The emulsion detector concept follows largely the current design of the FASER $\nu$  Experiment [12]. It consists of silver bromide crystals with diameters of 200 nm dispersed in gelatin media interleaved with a repeated

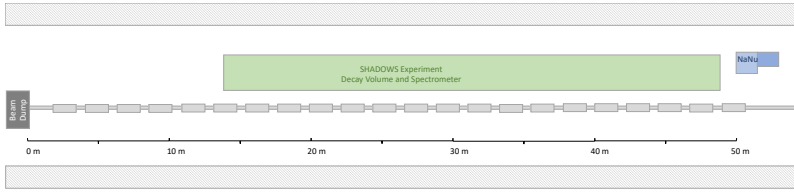


**Fig. 1.** Schematic drawing of the top-view on the location of the NaNu Experiment in the CERN North Area together with the future SHADOWS Experiment and the beam-line.

structure of absorber plates in which the actual charged current neutrino interactions occur. Emulsion detectors have a spatial resolution between 50 to 100 nm and can be interpreted as detectors with a huge density of active channels, i.e.  $10^{14}$  per  $\text{cm}^3$ . They are therefore perfectly suited for the study of short-lived particles with unique decay vertex structures. We propose to adopt the emulsion detector design of the successfully running FASER $\nu$  experiment, i.e. use emulsion films composed of two layers with a  $70 \mu\text{m}$  thickness which are separated by a  $200 \mu\text{m}$  thick plastic base. The emulsion films are interleaved by 1 mm tungsten plates due to their short radiation length. In total 560 tungsten plates with a total weight of the  $\approx 2.2$  t are foreseen. Given the significant multiple scattering effects within the tungsten plates, we foresee to place 40 emulsion tracking layers in the remaining 20 cm within the magnetic field, allowing for momentum measurements with higher precision. Those layers will be stabilized by thin aluminium plates, that are separated by 4 mm air gaps.

Since emulsion detectors cannot record timing information, all charged particles leave tracks and lead to significant pile-up. The emulsion detector is therefore complemented by six micromegas based tracking detectors with two-dimensional readout as well as a two-gap design, originally proposed in [13]. The thickness of these active detectors is about 15 mm and yields a spatial resolution of  $\approx 100 - 150 \mu\text{m}$  in two spatial dimensions with 3200 readout channels for each detector. The two-gap design allows in addition the reconstruction of complete tracklets with angular resolution of 0.02 rad.

The emulsion detector and magnet system is followed by a muon spectrometer consisting of three layers of the same micromegas-based technology as previously described but with larger dimensions of  $120 \times 70 \text{ cm}^2$  with 6080 readout channels per detector layer. The three layers are separated by 50 cm each, while the first layer is shielded in addition with a 20 cm iron layer to suppress hadronic particles. The active trigger system of NaNu makes use of plastic scintillators, which are located in the front as well as in the back of the emulsion layers, where they can be also used to veto muon signatures. In addition, the self-triggering capabilities of micromegas detectors can be used to record

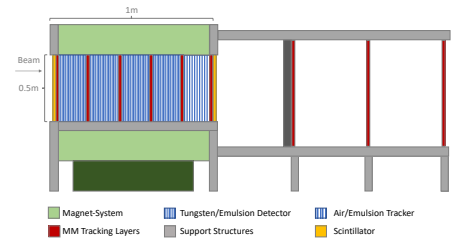


**Fig. 2.** Side-view of the NaNu experiment with its major components: emulsion detector, magnet and tracking stations.

events which only leave signatures within the emulsion target.

The location of the NaNu Experiment is foreseen 50 m after the beam dump, i.e. behind the SHADOWS experiment. The distance to the beam axis is chosen to minimize the expected muon background. Muons for the SHADOWS experiment are shielded by dedicated magnetized iron blocks. The expected muon background for  $4 \times 10^{19}$  proton on target in the transverse plane to the beam line is shown in Figure 3. The neutrino flux and the neutrino energies increase when moving towards the beam-line, however, also the muon-flux increases significantly. It is typically assumed that the reconstruction algorithms of emulsion detectors can handle  $\approx 10^6$  tracks per  $\text{cm}^2$ . The position of NaNu in the transverse plane was therefore optimized to be closest as possible to the beam-line, but the number of  $10^6$  muons per  $\text{cm}^2$  per year operation is not exceeded. This implies an optimal location of NaNu in the transverse plane with the coordinates  $x_1 = 1\text{m}$  to  $x_2 = 1.5\text{m}$  and  $y_1 = 1.0\text{m}$  and  $y_2 = 1.4\text{m}$ .

### 3 Neutrino Fluxes

Tau-neutrinos passing through the NaNu detector stem primarily from mesonic decays of  $D_s \rightarrow \tau\nu_\tau$ , together with a high rate of  $\nu_\mu$  and  $\nu_e$  neutrinos, which appear as decay products of charmed hadrons and soft pions and kaons. Our estimate of neutrino fluxes is based in studies of PYTHIA8 [14] and the GENIE program [15] and then cross-checked with the published studies of the Scattering and Neutrino Detector (SND) of the SHIP experiment [7, 8, 16]. The SND detector is assumed to be placed about 35 m after the interaction point, directly following the beamline. Its neutrino interaction target has a transverse size of  $0.8 \times 0.8 \text{ m}^2$ , a depth of  $\approx 1$  m and consists of passive absorber material interleaved with 19 emulsion and 19 tracking planes.

Since the production processes of neutrinos is the same for SND as for NaNu, the kinematic distributions of the produced neutrinos is equivalent for both experimental setups. However, the differences of the expected number of neutrino interactions are due to the different location, the different size as well as the different assumed number of protons on target.

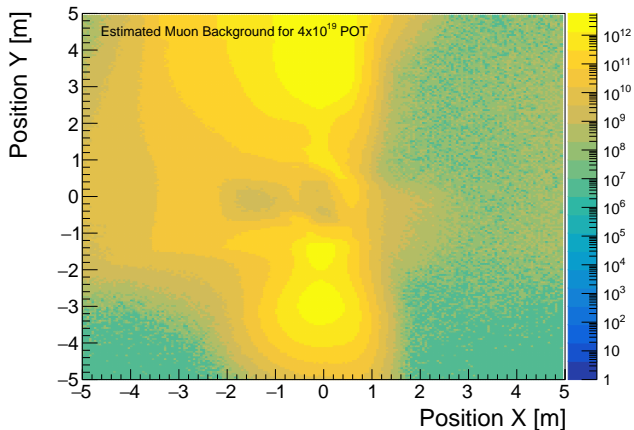


**Fig. 3.** Estimated muon background in the transverse plane to the beam axis at a distance of 50m after the beam dump for the expected  $4 \times 10^{19}$  protons on target.

Flavor	$\langle E \rangle$	Interactions ( $4 \times 10^{19}$ POT)
$\nu_e$	$\approx 16$ GeV	$16.6 \times 10^3$
$\nu_\mu$	$\approx 20$ GeV	$60.8 \times 10^3$
$\nu_\tau$	$\approx 27$ GeV	$0.6 \times 10^3$
$\bar{\nu}_e$	$\approx 13$ GeV	$3.9 \times 10^3$
$\bar{\nu}_\mu$	$\approx 16$ GeV	$13.5 \times 10^3$
$\bar{\nu}_\tau$	$\approx 32$ GeV	$0.4 \times 10^3$

**Table 1.** Expected energy range of neutrinos and number of neutrino interactions within the NaNu detector.

In four years of operation, we assume to have collected data corresponding to  $5 \times 10^{19}$  POT, i.e. a factor of 4 less compared to SND assumptions. The amount of passive absorber material also is significantly smaller for NaNu with a volume of  $0.11 \text{ m}^3$  and a weight of 2.2 t, yielding a further reduction by a factor of 3.3. Most important, however, is the difference in the actual location. PYTHIA8 [14] was used to estimate the kinematic distributions of all neutrino flavours after the initial proton-proton interactions. The angular distributions for electron, muon, and tau neutrinos is shown in Figure 4. In addition, the neutrino energy dependence on the neutrino interaction cross-sections have to be considered. In fact, the average neutrino energy reduces by up to 30 GeV, depending on the neutrino flavour, when placing the NaNu Detector with a distance of 1.5 to 2.0 m to the beam axis, implying significant lower cross-section in comparison to more high energetic neutrinos. The expected neutrino interactions in the NaNu detector due to its position is expected to be therefore reduced by a factor of 0.1 for electron neutrinos, and by a factor of 0.2 for muon and tau neutrinos. The final estimates of expected neutrino interactions per flavor are summarized in Table 1.

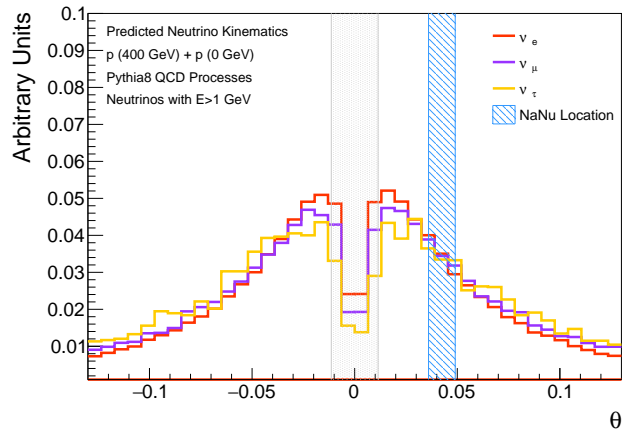


**Fig. 4.** Normalized angular distributions of neutrinos with  $E > 1$  GeV produced in 400 GeV proton beam collisions on a fixed proton target using PYTHIA8. The location of NaNu is indicated as blue shaded area.

## 4 Detector Simulation and Neutrino Identification

The NaNu detector concept has been implemented in GEANT4 [17] while the primary neutrino interactions with the passive detector material have been simulated via the GENIE program. It should be noted that the theoretical uncertainties on the actual neutrino fluxes as well as the hadronization model are typically larger than the experimental uncertainties involved in the following studies.

Neutrino interactions of all flavours require at least two tracks with an energy of 1 GeV associated to a common vertex with an impact parameter smaller than  $10 \mu\text{m}$ , one stemming from the lepton, the other(s) from the recoil of the nucleus. Tracks with larger impact parameters are treated as seed candidates for a secondary vertex. Secondary vertices can be defined via kinks on their corresponding tracks w.r.t. to the primary tracks as well as a by displacement of more than  $20 \mu\text{m}$  to the primary vertex. Primary and secondary decay vertices are searched for in all emulsion layers of NaNu except those close to the downstream tracking layers with a 1 cm margin. This reduces the acceptance of the NaNu detector by approximately 5%.

Electron neutrino interactions are identified by the characteristic electromagnetic showers of the electron as shown in Figure 5. A 90% detection efficiency is assumed, in line with studies of similar neutrino experiments. Given the short electron tracks, no charge measurement is possible. In total, we expect about 18 000 reconstructed electron neutrino events in the NaNu detector.

Muon neutrino interactions (Figure 5) can be identified by a primary vertex in the emulsion layer with one long track leaving the vertex. The curvature of the track in the magnetic field allows for a momentum

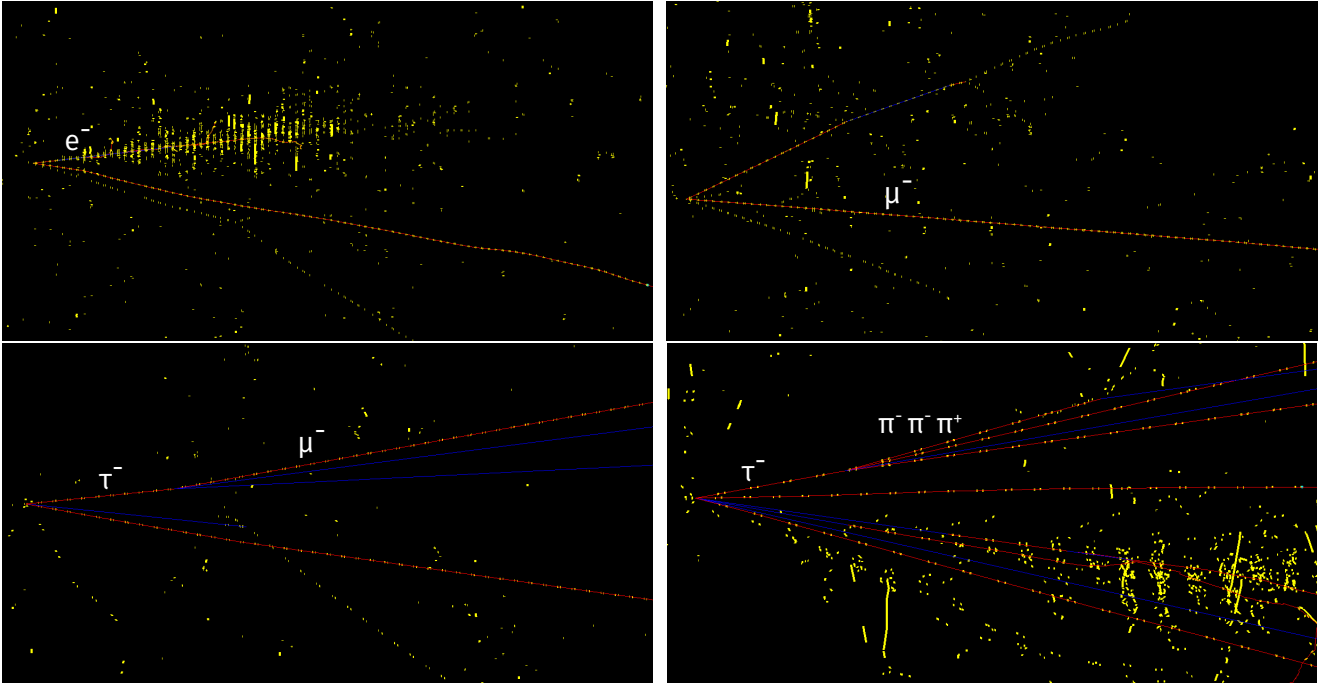


**Fig. 5.** Event Displays of the primary and secondary particle trajectories of electron neutrino (upper left) and muon neutrino (upper right) interactions with the NaNu Detector. Two example of tau neutrino interactions are shown in the lower row in the muonic decay channel (left) and the  $\tau \rightarrow \pi^+ \pi^- \pi^-$  decay channel (right). The charged (neutral) particles are indicated by red (blue) lines. Only particles with momenta larger than 1 GeV are shown.

measurement, using a combination of tracklets in the emulsion layers, the tracking layers as well as the muon spectrometer. The main sensitivity on the momentum comes from the measurements in the emulsion tracking layers in the last 20 cm of the magnetic field as well as from the muon spectrometer, since muons are subject to significant multiple scattering in the upstream passive detector layers. The expected momentum resolution for muon tracks in the NaNu detector has been estimated using a full GEANT4 simulation and is shown for 5 and 10 GeV muons in Figure 6. The resulting charge identification is correct in more than 98% of all recorded muon neutrino events. Assuming an 80% identification efficiency of the muons in the active tracking layers, we expect 40 000 and 10 000 reconstructed muon neutrino and anti-muon neutrino events, respectively. In fact, muon neutrino interactions could – in principle – be reconstructed using the active micromegas-based tracking detectors in standalone mode, if the primary muon neutrino interaction happens close the tracking layer and thus leaving a distinct signature of the recoil tracks of the nucleus. Detailed studies on this aspect are still ongoing.

The event topology of tau neutrino interactions depends on the subsequent decay of the tau lepton and, hence, the presence of a secondary vertex. The secondary vertex is expected to be reconstructed with an efficiency of  $\approx 60\%$ . Tau decays to electrons or muons yield a kink between the original tau track and the subsequent electron or muon tracks. The decay leptons can

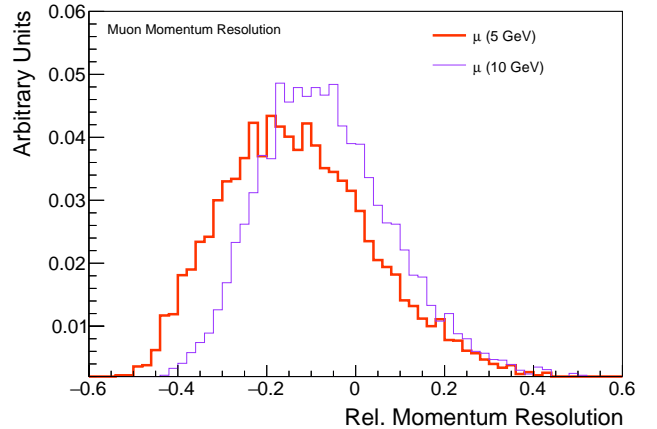


**Fig. 6.** Relative momentum resolution for muons with an energy of 5 and 10 GeV.

be identified as described above. The hadronic tau decays are identified by their short-lived decays and distinguished by the number of charged hadrons in the final state, i.e. into one or three charged pions. The three-pion decay has a unique topology, while the one-pion decay has a similar vertex structure as the muonic decay, however with a shorter track-length of 12.5 cm. This allows also for a momentum measurement using the tracking information within the magnetic field, where a significant better momentum resolution is achieved for tau-decays that happen close to end of the passive

emulsion detector layers. While studies on the momentum resolution for pions are still ongoing, preliminary results show that a correct charge identification is possible in more than 50% for all  $\tau \rightarrow h$  decays, with a false charge identification rate of 10%. The total number of reconstructed  $\nu_\tau$  and  $\bar{\nu}_\tau$  interactions at NaNu is nearly 500 events, detailed in Table 2 together with the efficiency losses at various stages of the identification. So far, only the charge identification in the muon and single-hadron decay topologies have been studied. Neglecting a possible charge identification in the electron and three hadron final state, we expect to identify 100  $\nu_\tau$  and 60  $\bar{\nu}_\tau$  interactions at NaNu for  $5 \times 10^{19}$  POT.

The main background in the tau lepton identification is due to the charm hadron production in  $\nu_\mu$  interactions via charged current interactions in the passive detector material. The subsequent decay topology of those hadrons has a similar decay topology as the tau decays when the primary lepton is not correctly identified. Hence the performance of the muon identification system is crucial for the background rejection. Given a larger reduction of the  $\nu_\mu$  interaction rate compared to SND@SHIP, we expect also a similar or even smaller background contribution in the  $\nu_\tau$  identifications.

## 5 Expected Physics Reach

The number of identified  $\nu_\tau$  and  $\bar{\nu}_\tau$  interactions in NaNu exceeds the previous statistics by nearly two orders of magnitude, allowing for a  $\bar{\nu}_\tau$  observation during the first year of data taking already. Beyond the first experimental observation of anti-tau neutrinos, neutrino interaction cross-sections of all flavours in the energy regime between 5 and 50 GeV can be measured with statistical and experimental uncertainties below 10%. The NaNu datasets provide therefore a unique opportunity to test lepton universality in neutrino interactions. All cross-section measurements are typically limited by the uncertainties on the initial neutrino flux. However, those uncertainties are of similar size in all neutrino collider experiments.

As mentioned in the previous section, the  $\bar{\nu}_\mu$  interactions in the passive detector material lead to significant charm hadron production, allowing to probe the strange quark content of the nucleon. Assuming a similar charm reconstruction efficiencies as SND@SHIP, we expect  $\approx 2 \times 10^3$  identified charm hadrons in NaNu, adding significantly to the exciting data-sets, potentially allowing to constrain further the parton distribution functions of protons.

Similarly to the determination of the upper limit for the magnetic moment of the tau neutrino by the DONUT Collaboration [4, 18], a study on the  $\nu_\tau$  magnetic moment can be performed at NaNu. Assuming similar systematic uncertainties but significantly improved statistics, it is expected to lower the upper limit by a factor of two to  $2 \times 10^{-7} \mu_B$ . The potential impact

of the NaNu datasets on the study of the  $F_4$  and  $F_5$  structure functions has still to be studied.

## 6 Estimated Costs

The existing dipole magnet (MNP 22/B) is the baseline choice for the magnet-system of the NaNu experiment. While it should be fully functional, it was not in active use in the past years and certain repair and refurbishing costs might arise. Those are estimated to not exceed 100 k€. The weight of the emulsion detector system requires a dedicated support frame, which allows an easy access for replacing the emulsion layers. Based on the support frame costs of the FASER experiment, 30 k€ should be sufficient to build the support frame.

The costs of the emulsion detector, including gel and film as well as additional infrastructure such as chemicals and tooling are estimated based on the costs of the FASER $\nu$  experiment [12] and scaled to the larger emulsion detector volume. The costs of the tungsten plates, which will be used as absorber material, is conservatively estimated using current market prices. The corresponding costs are summarized in Table 3.

The micromegas-based tracking chambers can be produced by the CERN workshops with a preliminary cost estimate of 100 k€ in total. The readout system will be based on the VMM-2 chipset [19], yielding overall costs of 280 k€. Additional costs for the veto plastic scintillators, the gas-system, the high-voltage supply as well as the basic computing infrastructure amount to 100 k€, resulting in overall estimated costs of the NaNu experiment of 1960 k€.

## 7 Summary

We proposed a cost effective experiment to study neutrino interactions at the SPS collider in an energy range of 20 to 60 GeV with a focus of tau neutrinos. The NaNu Experiment can be realized in the North Area of CERN between the future SHADOWS and HIKE Experiments and is based on well established technologies. The first experimental distinction of tau and anti-tau neutrinos can be already achieved with the first year of data taking. Furthermore, new upper bounds on the anomalous magnetic moment of tau neutrino are expected as well as precise neutrino cross-section measurements of all flavors. This study should mainly serve as a proof of concept and more detailed studies on the physics reach as well as the final detector concept are necessary. Most performance estimates have to be treated as preliminary. However, it becomes evident, that tau neutrino physics can be successfully conducted also off-beam axis in parallel to the operation of the SHADOWS experiment. More investments on the additional (and dedicated) muon shielding would allow to bring the NaNu detector closer to the beam-line might even allow to

	$\tau \rightarrow e$	$\tau \rightarrow \mu$	$\tau \rightarrow h(\pi^\pm)$	$\tau \rightarrow 3h(3\pi^\pm)$	$\bar{\tau} \rightarrow e$	$\bar{\tau} \rightarrow \mu$	$\bar{\tau} \rightarrow h(\pi^\pm)$	$\bar{\tau} \rightarrow 3h(3\pi^\pm)$
BR	0.17	0.18	0.46	0.12	0.17	0.18	0.46	0.12
Geometrical	0.9	0.9	0.9	0.9	0.9	0.9	0.9	0.9
Decay search	0.6	0.6	0.6	0.6	0.6	0.6	0.6	0.6
PID	1.0	0.8	0.9	0.9	1.0	0.8	0.9	0.9
Total Events	50	50	150	40	30	30	100	30

**Table 2.** Overview of various tau decay channels including their branching ratio (BR) together with the efficiencies of various selection and identification criteria. The last row indicated the expected number of reconstructed  $\nu_\tau$  events within NaNu.

Support Structure	30 k€
Magnet Refurbishment	100 k€
Emulsion Detector (Gel + Film)	600 k€
Emulsion Film Production Costs	100 k€
Infrastructure (chemicals, tools, racks)	50 k€
Tungsten Plates (2400 kg)	600 k€
Small Micromegas Tracking Stations (6x)	60 k€
Large Micromegas Tracking Stations (3x)	40 k€
Micromegas Readout System (VMM chip)	280 k€
Veto Plastic Scintillators	20 k€
Gas-System	30 k€
High-Voltage Supply	20 k€
Computing	30 k€
<b>Total</b>	<b>1,960 k€</b>

**Table 3.** Overview of the expected costs for the NaNu Experiment. The costs for the emulsion detector as well as the production costs cover one year of running, allowing for a first observation of anti-tau neutrino events.

increase the expected signal yields by a factor of 2-5. It should be noted that the envisioned energy range is complementary to the neutrino program of FASER-2 and even a common development of baseline technology could be envisioned.

## Acknowledgement

We thank Alfons Weber for the fruitful discussions during the preparation of this document, Sam Zeller for her help on the neutrino-interaction cross-sections as well as Akitaka Ariga for his input on the emulsion detector system. Special thanks also go to Florian Stummer for the muon background studies. This proposal would not have been possible without the support of the PRISMA<sup>+</sup> Cluster of Excellence as well as the ERC Grant Light@LHC.

## References

1. R. M. Abraham, et al., Tau neutrinos in the next decade: from GeV to EeV, *Journal of Physics G: Nuclear and Particle Physics* 49 (11) (2022) 110501. [arXiv:2203.05591](#), [doi:10.1088/1361-6471/ac89d2](#).
2. A. Ariga, et al., FASER’s physics reach for long-lived particles, *Phys. Rev. D* 99 (9) (2019) 095011. [arXiv:1811.12522](#), [doi:10.1103/PhysRevD.99.095011](#).
3. C. Ahdida, et al., SND@LHC - Scattering and Neutrino Detector at the LHC, Tech. Rep. CERN-LHCC-2021-003, LHCC-P-016, CERN, Geneva (2021).
4. K. Kodama, et al., Observation of tau neutrino interactions, *Phys. Lett. B* 504 (2001) 218–224. [arXiv:hep-ex/0012035](#), [doi:10.1016/S0370-2693\(01\)00307-0](#).
5. N. Agafonova, et al., Observation of a first  $\nu_\tau$  candidate in the OPERA experiment in the CNGS beam, *Phys. Lett. B* 691 (2010) 138–145. [arXiv:1006.1623](#), [doi:10.1016/j.physletb.2010.06.022](#).
6. R. L. Workman, Others, Review of Particle Physics, *PTEP* 2022 (2022) 083C01. [doi:10.1093/ptep/ptac097](#).
7. M. Anelli, et al., A facility to Search for Hidden Particles (SHiP) at the CERN SPS (CERN-SPSC-2015-016, SPSC-P-350) (2015). [arXiv:1504.04956](#).
8. C. Ahdida, et al., SHiP Experiment - Progress Report, Tech. Rep. CERN-SPSC-2019-010, SPSC-SR-248, CERN, Geneva (2019).
9. W. Bai, M. H. Reno, Prompt neutrinos and intrinsic charm at SHiP, *JHEP* 02 (2019) 077. [arXiv:1807.02746](#), [doi:10.1007/JHEP02\(2019\)077](#).
10. W. Baldini, et al., SHADOWS (Search for Hidden And Dark Objects With the SPS): Expression of Interest, Tech. Rep. CERN-SPSC-2022-006, SPSC-EOI-022, CERN, Geneva (2022).
11. E. Cortina Gil, et al., HIKE, the High Intensity Kaon Experiments at the CERN SPS: Letter of Intent, Tech. Rep. to be published.
12. H. Abreu, et al., Detecting and Studying High-Energy Collider Neutrinos with FASER at the LHC, *Eur. Phys. J. C* 80 (1) (2020)

61. [arXiv:1908.02310](#), [doi:10.1140/epjcs/s10052-020-7631-5](#).
13. B. Brickwedde, A. DÜdler, M. Schott, E. Yildirim, Design, Construction and Performance Tests of a Prototype MicroMegas Chamber with Two Read-out Planes in a Common Gas Volume, *Nucl. Instrum. Meth. A* 864 (2017) 1–6. [arXiv:1610.09539](#), [doi:10.1016/j.nima.2017.04.010](#).
14. C. Bierlich, et al., A comprehensive guide to the physics and usage of PYTHIA 8.3 (3 2022). [arXiv:2203.11601](#).
15. C. Andreopoulos, et al., The GENIE Neutrino Monte Carlo Generator, *Nucl. Instrum. Meth. A* 614 (2010) 87–104. [arXiv:0905.2517](#), [doi:10.1016/j.nima.2009.12.009](#).
16. S. Alekhin, et al., A facility to Search for Hidden Particles at the CERN SPS: the SHiP physics case, *Rept. Prog. Phys.* 79 (12) (2016) 124201. [arXiv:1504.04855](#), [doi:10.1088/0034-4885/79/12/124201](#).
17. S. Agostinelli, et al., GEANT4—a simulation toolkit, *Nucl. Instrum. Meth. A* 506 (2003) 250–303. [doi:10.1016/S0168-9002\(03\)01368-8](#).
18. R. Schwienhorst, et al., A New upper limit for the tau - neutrino magnetic moment, *Phys. Lett. B* 513 (2001) 23–29. [arXiv:hep-ex/0102026](#), [doi:10.1016/S0370-2693\(01\)00746-8](#).
19. G. Iakovidis, VMM - An ASIC for micropattern detectors, *EPJ Web Conf.* 174 (2018) 07001. [doi:10.1051/epjconf/201817407001](#).